

NMR Strategy for Determining Xaa-Pro Peptide Bond Configurations in Proteins: Mutants of Staphylococcal Nuclease with Altered Configuration at Proline-117[†]

Andrew P. Hinck,[‡] Eric S. Eberhardt, and John L. Markley*

Department of Biochemistry, College of Agricultural and Life Sciences, University of Wisconsin,
420 Henry Mall, Madison, Wisconsin 53706

Received May 5, 1993; Revised Manuscript Received August 20, 1993*

ABSTRACT: A general approach has been developed for configurational analysis (*cis* or *trans*) of Xaa-Pro peptide bonds in proteins. This approach, which entails selective ¹³C labeling of Xaa and Pro residues in the protein and isotope-edited NMR, has been applied to mutants of staphylococcal nuclease with suspected altered configurations of the Lys¹¹⁶-Pro¹¹⁷ peptide bond. The technique for monitoring proline configurations is based on differences in interproton distances between the H^α of residue Xaa and the proline H^δ or H^α protons. Short (<2.5 Å) Xaa H^α-Pro H^δ interproton distances are diagnostic for the *trans* configuration, whereas short (<2.5 Å) Xaa H^α-Pro H^α interproton distances are diagnostic for the *cis* configuration. Biosynthetic incorporation of [α-¹³C]Xaa and [δ-¹³C]proline facilitates detection of *trans* Xaa-Pro peptide bonds, whereas incorporation of [α-¹³C]Xaa and [α-¹³C]proline facilitates detection of *cis* Xaa-Pro peptide bonds. Provided that the Xaa-Pro peptide bond is unique within the protein sequence, symmetric off-diagonal NOE cross peaks in the isotope-edited NOE spectrum allow for simultaneous chemical shift assignment and determination of the prolyl peptide bond geometry. We have used this technique to determine the predominant configuration of the Lys¹¹⁶-Pro¹¹⁷ peptide bond in recombinant V8 staphylococcal nuclease A (H124L) and two of its single amino acid mutants (D77A+H124L and G79S+H124L). The results are consistent with conclusions reached on the basis of indirect arguments concerning changes in the chemical shifts of histidine ¹H^{ε1} NMR signals. The Lys¹¹⁶-Pro¹¹⁷ peptide bond was found by this direct isotope-edited NOE method to be predominantly *cis* in H124L but predominantly *trans* in D77A+H124L and G79S+H124L. However, when a saturating amount of an inhibitor (pdTp plus Ca²⁺) was added to either D77A+H124L or G79S+H124L, the peptide bond became predominantly *cis*.

The propensity of proline residues to form *cis* peptide bonds in folded proteins is unique among the twenty common amino acids. Structurally, *cis* Xaa-Pro peptide bonds, which are essential to the formation of type VI reverse turns, provide an important means of reversing the chain direction and allowing the backbone to pack onto itself. *Trans* Xaa-Pro peptide bonds introduce steric interactions between the pyrrolidine ring δ-position and the preceding residue. This raises the free energy of the *trans* form and effectively diminishes the net free energy difference between the *cis* and *trans* configurations relative to non-proline-containing peptide bonds, and it provides one explanation for the common occurrence of *cis* prolines among protein structures (Wüthrich & Grathwohl, 1974).

The relatively low activation barrier for isomerization, ~13 kcal/mol (MacArthur & Thornton, 1991), combined with the small energy difference between *cis* and *trans* Xaa-Pro peptide bond configurations provides a mechanism for slow interconversion of alternative forms of proteins in the folded and unfolded states. The role of prolyl *trans* to *cis* isomerization in the kinetics of protein folding reactions has been thoroughly investigated, and it is now widely accepted that peptide bond isomerization provides a mechanism for slow steps in protein folding reactions (Kim & Baldwin, 1982). The structural and functional consequences of peptide bond

isomerization in folded proteins has been characterized less thoroughly (Chazin et al., 1989; Alexandrescu et al., 1989; Evans et al., 1987; Ludwig & Luschinsky, 1992), but the strict evolutionary conservation of some proline residues (Barlow & Thorton, 1988; Langsetmo et al., 1989) and the recent discovery of widely abundant proteins with prolyl peptide bond isomerase activity suggest that peptide bond isomerization may play an important role in protein structure and function. Suggestive examples include the sodium pump of *Escherichia coli* and the protein disulfide isomerase/thioredoxin class of enzymes. Several lines of evidence now suggest that isomerization of a proline residue, which is centrally located in a transmembrane α-helix of the sodium pump, is synchronous with ion translocation (Brandl & Deber, 1986). In *E. coli* thioredoxin, it has been suggested that proline isomerization may be linked thermodynamically with the cleavage and reformation of the active site disulfide (Langsetmo et al., 1989).

Staphylococcal nuclease (nuclease) is the best characterized protein in which isomerization of a prolyl peptide bond in the folded state has been studied. The existence of conformational substates in staphylococcal nuclease was first observed in the splitting of the well-resolved histidine ¹H^{ε1} resonances (Markley et al., 1970). Mechanisms for conformational heterogeneity in staphylococcal nuclease have been attributed to isomerization about the Lys¹¹⁶-Pro¹¹⁷ (Fox et al., 1986; Alexandrescu et al., 1989) and His⁴⁶-Pro⁴⁷ peptide bonds (Loh et al., 1991). Changes in the signals from His⁸, His¹²¹, and His¹²⁴ are thought to report on isomerization of the Lys¹¹⁶-Pro¹¹⁷ peptide bond, whereas changes in the signals from His⁴⁶ report on isomerization of the His⁴⁶-Pro⁴⁷ peptide bond

[†] A.P.H. was supported by Molecular Biophysics Training Grant GM08293 (NIH), and E.S.E. is a Wharton Predoctoral Fellow. This work was supported by NIH Grant GM35976.

* Author to whom correspondence should be addressed.

[‡] Present address: Department of Chemistry, University of Wisconsin, 1101 University Ave., Madison, WI 53706.

• Abstract published in *Advance ACS Abstracts*, October 15, 1993.

(Alexandrescu et al., 1989; Loh et al., 1991). In wild-type nuclease (WT),¹ the predominant configuration (a_1) of the Lys¹¹⁶-Pro¹¹⁷ peptide bond is presumed to be *cis* (85%), whereas the minor configuration (a_2) is presumed to be *trans* (15%).² For the His⁴⁶-Pro⁴⁷ peptide bond, the major configuration (b_1) is presumed to be *trans* (80%), whereas the minor configuration (b_2) is presumed to be *cis* (20%). The two conformational transitions are not coupled to one another, so that four separate species are populated in solution; a_1b_1 , a_1b_2 , a_2b_1 , and a_2b_2 .

Evidence that links proline isomerization to conformational heterogeneity of the enzyme in solution has come from magnetization transfer NMR spectroscopy. Not only were the observed rates for interconversion of a_1 and a_2 and b_1 and b_2 forms consistent with those expected for proline isomerization (Evans et al., 1989; Alexandrescu et al., 1989; Loh et al., 1991); two unfolded forms of the protein were also detected on the basis of magnetization transfer from His¹²¹. Additional support has come from site-directed mutagenesis experiments in which proline to glycine mutants have been constructed at both of these positions. The P117G mutant eliminated heterogeneity at His⁸, His¹²¹, and His¹²⁴ (Evans et al., 1987; Alexandrescu et al., 1990) and left His⁴⁶ unaffected; by contrast the P47G+H124L mutant eliminated the heterogeneity at His⁴⁶ but left His⁸ and His¹²¹ undisturbed (Loh et al., 1991).

In all X-ray structures of WT, both in the ternary complex with Ca²⁺ and pdTp and in their absence, the Lys¹¹⁶-Pro¹¹⁷ peptide bond has been modeled only in the *cis* configuration (Cotton et al., 1979; Loll & Lattman, 1989; Hynes & Fox, 1991). In solution, the configuration of Pro¹¹⁷ has been investigated by two previous NMR studies. In the first, [γ -¹³C]-Pro was incorporated into the wild-type protein, and proline ¹³C chemical shifts were monitored by the 2D HMQC experiment (Stanczyk et al., 1989). On the basis of the typical 3 ppm upfield shift of the C γ resonances in model peptides in the *cis* configuration (Torchia, 1984) and on comparison of ¹³C chemical shifts in the spectrum of the wild-type protein with those of the P117G mutant, the Lys¹¹⁶-Pro¹¹⁷ peptide bond was identified as *cis*. A more thorough investigation

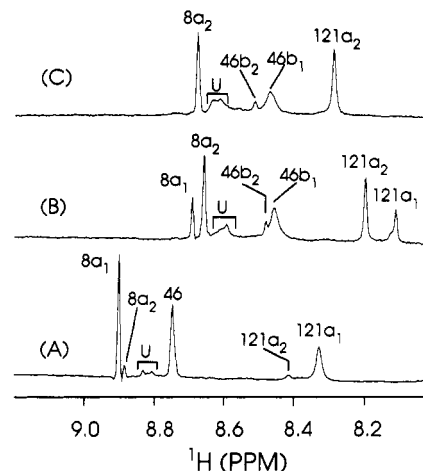


FIGURE 1: Histidine ¹H^α region of the ¹H NMR spectrum of three staphylococcal nuclease variants: (A) H124L, (B) G79S+H124L, and (C) D77A+H124L. Spectra were acquired at 38 °C on a Bruker AM500 spectrometer equipped with a variable-temperature ¹H probe. Histidine peaks a_1 and a_2 report on the peptide bond configuration of Lys¹¹⁶-Pro¹¹⁷, and peaks b_1 and b_2 report on the two peptide bond configurations of His⁴⁶-Pro⁴⁷. Peaks arising from histidines in the unfolded state (indicated by U) were ascertained by temperature-titration experiments. The a_1 and a_2 forms were assigned (Alexandrescu et al., 1990) on the basis of their response to the addition of pdTp (Figure 6), whereas the b_1 and b_2 assignments were by comparison to the wild-type protein (Loh et al., 1991).

was reported by Torchia and co-workers (1989), who incorporated [α -¹³C]Pro and [γ -¹³C]Pro into recombinant nuclease³ and used existing backbone and side-chain assignments to completely assign the proline spin systems. Interproton distances, manifested in NOE spectra of isotopically enriched [α -¹³C]Pro samples, characteristic of the *cis* geometry (Wüthrich, 1986) were identified between the H α of Pro¹¹⁷ and the H α of the preceding residue, Lys¹¹⁶ (Torchia et al., 1989).

In the course of exploring the sequence code that specifies a predominantly *cis* Lys¹¹⁶-Pro¹¹⁷ peptide bond in nuclease, we have constructed a set of single amino acid mutants in which the equilibrium constant for isomerization about the Lys¹¹⁶-Pro¹¹⁷ peptide bond is shifted toward *trans* (Alexandrescu et al., 1989; Hinck, 1993). On the basis of histidine splittings, the mutant in which glycine-79 is replaced by serine contains 69% of one configuration (presumably *trans*), whereas the mutant in which aspartic acid-77 is replaced by alanine contains >99% of a single configuration (presumably *trans*; Figure 1).

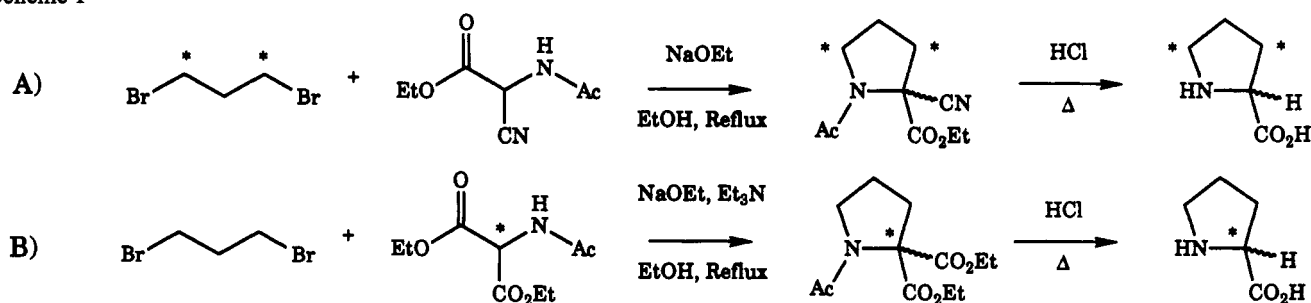
Our goal in this study was to develop a direct method for correlating the observed histidine splittings with the configuration about the Lys¹¹⁶-Pro¹¹⁷ peptide bond. The previous NMR studies of the Lys¹¹⁶-Pro¹¹⁷ peptide bond configuration discussed above only examined wild-type (or related) nuclease molecules in which >85% of the molecules had the *cis* configuration. No studies have provided direct evidence for a *trans* peptide bond in the alternate population. All inferences about the configuration of the Lys¹¹⁶-Pro¹¹⁷ peptide bond in mutants with altered populations of subspecies have come from indirect arguments such as the effect of pdTp binding on substrates detected by splitting of histidine signals (Fox et al., 1986; Alexandrescu et al., 1989; Markley et al., 1970).

¹ Abbreviations: HMQC, heteronuclear multiple quantum shift correlation; HMQC-NOE, the HMQC experiment with a combined NOE relay period; HSMQC, heteronuclear single and multiple quantum shift correlation; ω_1 IE-NOESY, an isotope-edited NOE experiment with heteronuclear editing in the first (indirectly observed) frequency dimension; IPTG, isopropyl β -D-thiogalactopyranoside; LB, Luria-Bertani bacterial growth medium; NAc-Lys-Pro-OMe, methyl N-acetyl-L-lysyl-L-prolinate; NMR, nuclear magnetic resonance; NOE, nuclear Overhauser effect; ppm, parts per million; pdTp, thymidine-3',5'-diphosphate; pH*, pH value of ²H₂O solutions uncorrected for the deuterium isotope effect; SDS-PAGE, sodium dodecyl sulfate-polyacrylamide gel electrophoresis; TFA, trifluoroacetic acid; THF, tetrahydrofuran; TSP, 3-(trimethylsilyl)-propionic-*d*₄ acid; WT, recombinant protein produced in *Escherichia coli* which is identical to the extracellular nuclease produced by the Foggi strain of *Staphylococcus aureus*; H124L, recombinant protein produced in *E. coli* which differs from WT by the substitution of leucine for histidine at position 124 (its sequence is identical to the extracellular nuclease produced by the V8 strain of *Staphylococcus aureus*); D77A+H124L, single amino acid mutant of H124L in which aspartic acid-77 is replaced by alanine; G79S+H124L, single amino acid mutant of H124L in which glycine-79 is replaced by serine; P117G, single amino acid mutant of WT in which proline-117 is replaced by glycine; P47G+H124L, single amino acid mutant of H124L in which proline-47 is replaced by glycine.

² Symbols a_1 and a_2 denote the major and minor conformational forms, respectively, of wild-type nuclease as detected by doubling of the ¹H^α signals from His⁸, His¹²¹, and His¹²⁴. Peaks a_1 and a_2 for mutant proteins have been assigned operationally (Alexandrescu et al., 1990) by their relative changes in intensity upon addition of Ca²⁺ and pdTp: the a_1 peaks increase at the expense of the corresponding a_2 peaks. Symbols b_1 and b_2 refer respectively to the major and minor conformational forms detected by splitting of the His⁴⁶ peak (Loh et al., 1991).

³ In comparison to WT, which contains six prolyl residues, the amino acid sequence of the recombinant nuclease used by Torchia et al. (1989) contained seven prolyl residues. Its sequence was identical to that of the nuclease isolated from the Foggi strain of *Staphylococcus aureus*, except for an N-terminal heptapeptide extension with the sequence M-D-P-T-V-Y-S.

Scheme 1



In the present work, we have used isotope-edited NOE methods to probe the configuration of the Lys¹¹⁶-Pro¹¹⁷ peptide bond directly, both in nucleases in which the peptide bond is expected to be largely *cis* and in single amino acid variants in which it is predicted to be largely *trans*. The results of this analysis agree with assignments made on the basis of perturbation by pdTp binding. The technique we have developed, however, is general and should be applicable to other small proteins, where it can be used to determine the possible role of prolyl peptide bond configuration in protein folding, stability, or mechanism of action.

EXPERIMENTAL PROCEDURES

Materials. K¹³CN and sodium [2-¹³C]acetate were purchased from Cambridge Isotope Laboratories (Woburn, MA). Sodium [1-¹³C]acetate was from Merck Stable Isotopes (Montreal, Canada). Trifluoroacetic anhydride, 2 M borane-dimethyl sulfide in THF, 1,3-dibromopropane, *N*-(δ-iodobutyl)phthalimide, and 48% HBr were purchased from Aldrich (Milwaukee, WI). Ethyl acetamidocyanoacetate (Aldrich) was recrystallized from ethanol before use. ²H₂O, 99.8% and 99.997%, was from Isotec (Miamisburg, OH) and Cambridge Isotope Laboratories, respectively. Thymidine 3',5'-diphosphate (pdTp) and 20% homogeneous SDS-PAGE gels for the Phastgel electrophoresis system were obtained from Pharmacia (Piscataway, NJ). IPTG was from Gold Bio-technology (St. Louis, MO); ultrapure CaCl₂ was from Alfa (Danvers, MA); and vitamin diet fortification mixture was from Nutritional Biochemical Corp. (Cleveland, OH). AG3-X4A anion-exchange resin was from BioRad (Richmond, CA). All other chemicals were of reagent grade or better and were used without further purification.

Chemical Syntheses. D,L-[3,5-¹³C]Proline and D,L-[2-¹³C]-proline were prepared in two steps by alkylation of malonic ester derivatives with 1,3 dibromopropane as shown in Schemes 1A and 1B, respectively. The necessary labeled precursors, 1,3-dibromo[1,3-¹³C]propane and diethyl [2-¹³C]acetamidomalonate were prepared in three and four steps, respectively, in overall yields of 47.5% and 43.4% (Schemes 1S and 2S in the supplementary material). 1,3-Dibromo[1,3-¹³C]propane was prepared by bromination of [1-¹³C]acetic acid followed by nucleophilic displacement with K¹³CN to yield diethyl [1,3-¹³C]malonate, which was subsequently reduced and brominated to yield 1,3-dibromo[1,3-¹³C]propane. Diethyl [2-¹³C]-acetamidomalonate was synthesized by bromination of [2-¹³C]acetic acid and subsequent CN⁻ displacement to yield diethyl [2-¹³C]malonate. Treatment of diethyl [2-¹³C]-malonate with HNO₂ yielded the oxime, which was catalytically reduced at high pressure and acylated, to form diethyl [2-¹³C]acetamidomalonate. Detailed descriptions for each of the transformations are provided in the supplementary material.

Molecular Biology. The DNA construct pTSN2cc encodes a protein (H124L) whose sequence, with the exception of an

N-terminal methionine residue, is identical to the extracellular nuclease isolated from the V8 strain of *Staphylococcus aureus* (Wang et al., 1990). The N-terminal methionine appears to be removed following protein synthesis. Site-directed variants of H124L (D77A+H124L and G79S+H124L) were generated as described by Royer et al. (1993). Both mutants were confirmed by double stranded DNA sequencing of the recombinant overproducing plasmids.

***E. coli* Proline and Lysine Auxotroph.** An auxotrophic strain of *E. coli*, which carried the genetic markers *proC*::Tn5, Δ(*putPA*), and *lysA* (Bachman, 1983) and the T7 RNA polymerase gene under control of the *lacUV5* promoter as a stable λ lysogen (Studier et al., 1989), was constructed by P1 transduction (Sternber & Maurer, 1991; Kleckner et al., 1991). The parent strain WG139, which was obtained as a gift from Dr. Janet Wood, University of Guelph, contained the markers *proC*::Tn5 and Δ(*putPA*). The *lysA* and T7 markers were introduced from donor strains, AT713 (CGSC #4529) and BL21(DE3) (Studier et al., 1989), which were modified with Tn10 insertions near the respective scorable markers: *acd*::Tn10 near *lysA* and *nadA*::Tn10 near T7. The P1 transductions were performed sequentially by the method of Miller (1977). Following each round of transduction, the strain was purified by streaking onto LB medium; single colonies were screened for the appropriate phenotype of interest, and tetracycline sensitivity was restored by plating onto Bochner plates (Bochner et al., 1980). The final construct was denoted WGTK1.

Isotopic Labeling. Selective ¹³C labeling of wild-type and mutant nucleases at all lysine and proline residues was accomplished biosynthetically. The appropriate nuclease overexpression vector was transformed into a strain of *E. coli* auxotrophic for both proline and lysine (WGTK1). The cells were grown as described previously by Royer et al. (1993) with the following changes: M9 medium (Sambrook et al., 1989) was substituted for LB medium which was supplemented with D,L-[2-¹³C]proline or D,L-[3,5-¹³C]proline (50 mg) and D,L-[2-¹³C]lysine (100 mg) along with each of the common amino acids at the levels recommended by Davis et al. (1980). In addition, 100 mg/L each of nicotinic acid and thiamine HCl and 5 mL of a saturated aqueous solution of vitamin diet fortification mixture were added. Protein purification was as previously described (Royer et al., 1993); purities were confirmed by electrophoresis on 20% homogeneous SDS-PAGE gels. The concentrations of wild-type and mutant nucleases were determined at 280 nm by using the previously determined extinction coefficient, ε = 1.56 × 10⁴ M⁻¹ cm⁻¹ (Cuatrecasas et al., 1967). Since the mutations studied do not involve aromatic residues, the extinction coefficient was assumed to remain constant.

NMR Spectroscopy. Synthetic products were characterized with a Bruker AM500 NMR spectrometer at ambient temperature. Proton chemical shifts in ²H₂O and CDCl₃ are reported relative to internal TSP (0 ppm) and residual CHCl₃

(7.15 ppm), respectively. Carbon chemical shifts of aqueous samples are reported relative to external dioxane (67.8 ppm); those of samples dissolved in CHCl_3 were measured relative to the chemical shift of CDCl_3 , which was assumed to have a chemical shift of 77.0 ppm relative to $(\text{CH}_3)_4\text{Si}$.

Protein samples were prepared for NMR spectroscopy as follows. The lyophilized salt-free protein was dissolved in 99.8% $^2\text{H}_2\text{O}$ (0.50 mL) and heated at 45 °C for 1 h in order to exchange labile protons. The pH* was adjusted to 5.50 with small aliquots of 1 M ^2HCl or 1 M KO^2H as needed, and the sample was lyophilized. The sample was dissolved next in 99.997% $^2\text{H}_2\text{O}$ (0.5 mL), and the lyophilization step was repeated. Then, the sample was dissolved in 99.997% $^2\text{H}_2\text{O}$ (0.5 mL) and transferred to an NMR tube. The concentrations of the unlabeled samples were 2.4 mM (H124L), 2.1 mM (G79S+H124L), and 1.85 mM (D77A+H124L). The concentrations of $[\alpha\text{-}^{13}\text{C}]\text{Pro}$ and $[\alpha\text{-}^{13}\text{C}]\text{Lys}$ isotopically enriched samples were 2.0 (H124L) and 2.5 mM (G79S+H124L). The concentrations of $[\beta,\delta\text{-}^{13}\text{C}]\text{Pro}$ and $[\alpha\text{-}^{13}\text{C}]\text{Lys}$ enriched samples were 3.2 (H124L) and 5.00 mM (D77A+H124L).

Solutions of inhibited isotopically enriched samples were prepared by adding 0.245 M pdTp in $^2\text{H}_2\text{O}$ at pH* 5.5 and 0.40 M CaCl_2 to give the desired protein: CaCl_2 :pdTp composition. The samples then were lyophilized and redissolved in the original volume of $^2\text{H}_2\text{O}$. The protein: CaCl_2 :pdTp composition for $[\alpha\text{-}^{13}\text{C}]\text{Lys}$ and $[\beta,\delta\text{-}^{13}\text{C}]\text{Pro}$ enriched D77A+H124L was 1:20:10; those for the three $[\alpha\text{-}^{13}\text{C}]\text{Lys}$ and $[\alpha\text{-}^{13}\text{C}]\text{Pro}$ enriched G79S+H124L samples were 1:1:0.5, 1:2:1, and 1:10:5.

Inhibitor titrations of unlabeled proteins were carried out by the addition of aliquots of 0.40 M CaCl_2 and 0.245 M pdTp dissolved in $^2\text{H}_2\text{O}$ at pH* 5.50. The initial protein concentrations were 2.1 mM for G79S and 1.85 mM for D77A. Ligand:protein ratios were calculated on the basis of the known initial volume and protein concentrations. NMR spectra were acquired at 32 °C on a Bruker AM500 spectrometer equipped with a variable-temperature ^1H probe.

Samples of ^{13}C isotopically enriched nuclease were analyzed by the HSMQC experiment (Zuiderweg, 1990), by a variation of the HMQC experiment with an additional ^1H - ^1H NOE relay period (HMQC-NOE) (Shon & Opella, 1989), and by an ω_1 half-filtered isotope-edited NOE (ω_1 IE-NOE) experiment (Otting & Wüthrich, 1990). The HMQC-NOE (A) and IE-NOE (B) pulse sequences were

(A) ^1H 90 ϕ_1 - Δ - $t_{1/2}$ -180 γ - $t_{1/2}$ - Δ - 90 ϕ_4 - τ_{mix} - 90 ϕ_5 - AQ (ψ)
 ^{13}C 90 ϕ_2 90 ϕ_3 GARP

(B) ^1H 90 ϕ_1 - Δ - 180 γ - Δ - $t_{1/2}$ - 90 ϕ_4 - τ_{mix} - 90 ϕ_5 - AQ (ψ)
 ^{13}C 90 ϕ_2 90 ϕ_3 GARP GARP

The phase cycles used in sequence A were $\phi_1 = (x)_4(-x)_4$; $\phi_2 = x, -x$; $\phi_3 = x, x, -x, -x$; $\phi_4 = (x)_{32}(-x)_{32}$; $\phi_5 = (x)_8(-y)_8(-x)_8(-y)_8$; and $\psi = (\Omega, \Theta, -\Omega, -\Theta, -\Omega, -\Theta, \Omega, \Theta)$, where $\Omega = x, -x, -x, x, -x, x, x, -x$ and $\Theta = y, -y, -y, y, -y, y, y, -y$. The phase cycles used in sequence B were $\phi_1 = x, x, -x, -x$; $\phi_2 = x, -x$; $\phi_3 = (x)_4(-x)_4(y)_4(-y)_4$; and $\psi = x, -x, -x, x, -x, x, x, -x, y, -y, -y, y, -y, y, y, -y$. ^{13}C decoupling was provided by a GARP (Shaka et al., 1983) modulation sequence during the acquisition period of both experiments and was also used during the t_1 evolution period of the IE-NOE sequence to eliminate effects due to ^1H - ^{13}C scalar coupling. The delay, Δ , was set to 4.5 ms, slightly shorter than optimal

for ^1H - ^{13}C $^1J_{\text{C-H}}$ coupling to compensate for rapid t_2 relaxation. Proton chemical shifts are reported relative to internal TSP (0 ppm); carbon chemical shifts are reported relative to external dioxane (67.8 ppm). Additional NMR parameters for the isotopically enriched samples are given in the figure captions.

Simulation of Interproton Distances. Energy minimization and molecular dynamics calculations were performed on the neutral dipeptide, NAc-Lys-Pro-OMe, *in vacuo*, with version 2.8 of the DISCOVER molecular modeling package (Biosym, San Diego, CA) implemented on a Silicon Graphics 4D 220 GTX workstation (Mountain View, CA). The torsion angle, ω , was fixed at 15° increments by applying a force of 1000 kcal rad $^{-2}$. After each incrementation of ω , the energy was minimized by applying 1000 cycles of steepest-descent minimization, followed by 1000 cycles of minimization with the Newton-Raphson algorithm and 15 ps of molecular dynamics at 450 K. During the last 10 ps of the dynamics, the interproton distances between lysine H^α and proline H^α , $\text{H}^{\delta 1}$, and $\text{H}^{\delta 2}$ were sampled every 0.1 ps. The means and standard deviations of these distances were calculated for each incrementation of ω between -180° and 180°.

RESULTS

Interproton Distances. Figure 2 shows selected interproton distances in the model peptide NAc-Lys-Pro-OMe as a function of the peptide bond configuration as modeled by molecular dynamics. When the peptide bond is *trans* ($\omega = \pm 180^\circ$), the Lys H^α -Pro H^α distance is >4.5 Å, and the Lys H^α -Pro $\text{H}^{\delta 1,2}$ distances are <2.6 Å. When the configuration is *cis*, the Lys H^α -Pro H^α distance is <2.6 Å, and the Lys H^α -Pro $\text{H}^{\delta 1,2}$ distances are >4.5 Å. Thus, observable Lys H^α -Pro H^α NOEs are expected only if the peptide bond is *cis*, and observable Lys H^α -Pro H^δ NOEs are expected only when the peptide bond is *trans*.

Isotope-Assisted Analysis. Four isotopically enriched samples were prepared and analyzed: H124L and G79S+H124L, both enriched with $[\alpha\text{-}^{13}\text{C}]\text{Lys}$ + $[\alpha\text{-}^{13}\text{C}]\text{Pro}$, and H124L and D77A+H124L, both enriched with $[\alpha\text{-}^{13}\text{C}]\text{Lys}$ + $[\beta,\delta\text{-}^{13}\text{C}]\text{Pro}$. In the HSMQC spectrum of $[\alpha\text{-}^{13}\text{C}]\text{Lys}$ and $[\alpha\text{-}^{13}\text{C}]\text{Pro}$ enriched H124L (Figure 4A), the $^{13}\text{C}^\alpha$ resonances from the six proline residues are clustered near 62.5 ppm, while those corresponding to the 23 lysine resonances range from 52 to 59 ppm. In the HMQC-NOE spectrum of the same protein under the same conditions (Figure 4B), NOEs are manifested as additional cross peaks which share the ^{13}C chemical shifts of ^1H - ^{13}C correlation cross peaks. One NOE cross peak at the Pro 117 $^{13}\text{C}^\alpha$ chemical shift has the same ^1H chemical shift as Lys 116 $^1\text{H}^\alpha$, and one NOE cross peak at the Lys 116 $^{13}\text{C}^\alpha$ chemical shift has the same ^1H chemical shift as Pro 117 H^α . The results of the ω_1 IE-NOESY experiment are presented in Figure 4C. As expected from the results of the HMQC-NOE experiment, symmetric off-diagonal cross peaks are found at the intersections of the Lys 116 H^α /Pro 117 H^α and Pro 117 H^α /Lys 116 H^α ^1H chemical shifts. These results provide conclusive evidence that the major configuration of the Lys 116 -Pro 117 peptide bond in nuclease H124L in the absence of active site ligands is *cis*.

$[\alpha\text{-}^{13}\text{C}]\text{Lys}$ and $[\beta,\delta\text{-}^{13}\text{C}]\text{Pro}$ enriched H124L was analyzed by the same repertoire of experiments just described (data not shown). In the HMQC-NOE and ω_1 IE-NOESY spectra, no NOEs were found between the H^α of Lys 116 and the Pro H^δ resonances or between the Pro H^δ resonances and the H^α of Lys 116 . These results are also consistent with a predominantly *cis* Lys 116 -Pro 117 peptide bond.

Results for $[\alpha\text{-}^{13}\text{C}]\text{Lys}$ and $[\alpha\text{-}^{13}\text{C}]\text{Pro}$ enriched D77A+H124L are presented in Figure 5. In the HSMQC

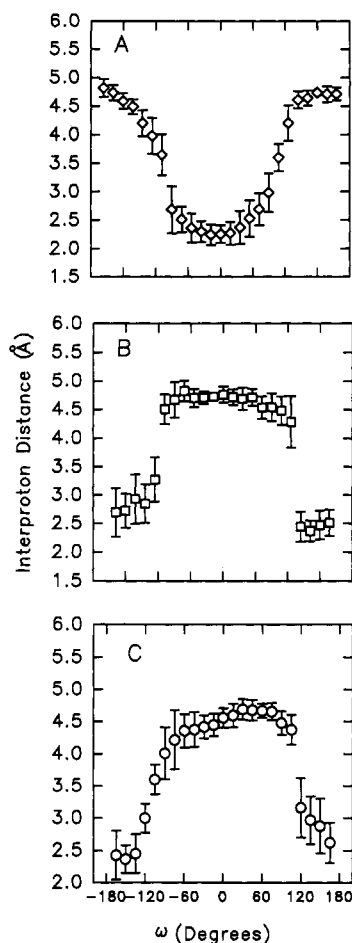


FIGURE 2: Three interproton distances in the dipeptide NAc-Lys-Pro-OMe as a function of rotation of the peptide bond dihedral angle, ω : (A) Lys H^α -Pro H^α , (B) Lys H^α -Pro $H^{\delta 1}$, and (C) Lys H^α -Pro $H^{\delta 2}$. The calculated distances were obtained by fixing ω with a force and by performing energy minimization and 15 ps of molecular dynamics. The calculated distances and associated errors were calculated from the mean and the standard deviation of the interproton vector sampled every 0.1 ps during the last 10 ps of molecular dynamics.

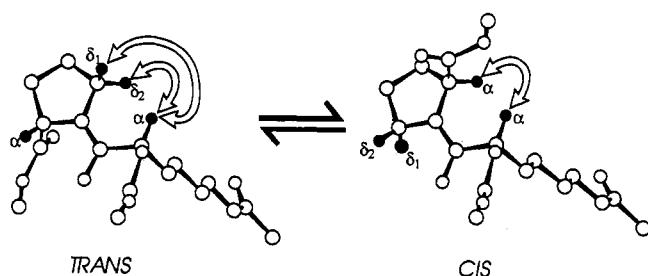


FIGURE 3: Ball and stick model of NAc-Lys-Pro-OMe in the *trans* and *cis* conformations with arrows indicating the uniquely observable strong NOEs in the two states.

spectrum of this mutant (Figure 5A), the Lys $^{13}C^\alpha$ resonances again fall in the 52–59 ppm range, while the Pro $^{13}C^\delta$ resonances are grouped near 49 ppm. In the ω_1 IE-NOESY spectrum (Figure 5C), several pairs of NOE cross peaks are visible above the diagonal with F_2 chemical shifts between 4.5 and 5.0 ppm originating from the interaction between Pro H^δ protons and H^α protons. Visible below the diagonal is just a single pair of NOEs which link Lys H^α to the two Pro H^δ nuclei. This pair is symmetric with a pair of peaks above the diagonal. Assignment of these NOEs to Lys $^{116}H^\alpha$ and Pro $^{117}H^{\delta 1}$ and $H^{\delta 2}$ protons is confirmed by the HMQC-NOE (Figure 5B). Two NOEs are present at the ^{13}C chemical shift of

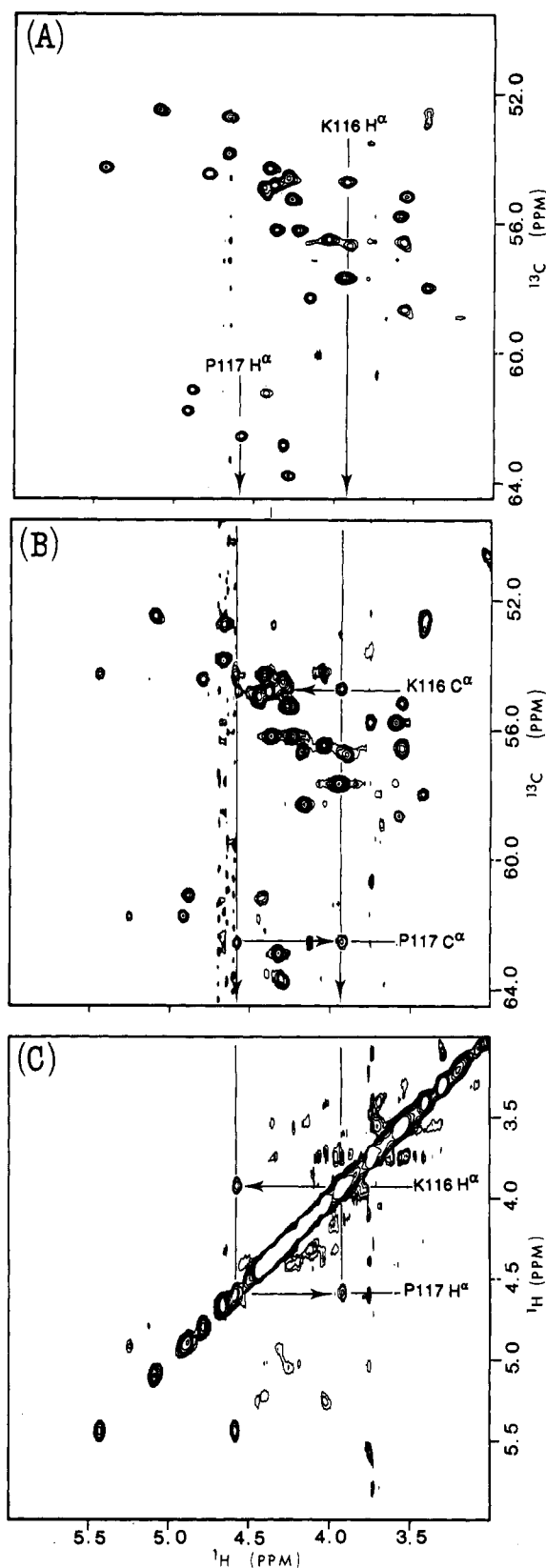


FIGURE 4: (A) HSMQC, (B) HMQC-NOE, and (C) ω_1 IE-NOESY spectra of $[\alpha\text{-}^{13}C]$ Lys and $[\alpha\text{-}^{13}C]$ Pro enriched H124L. The data were collected at 37 °C on a Bruker AM500 spectrometer equipped with a $^1H/^{13}C$ variable-temperature probe. The sweep widths in F_2 and F_1 for the HSMQC and HMQC-NOE experiments were 6024 and 3773 Hz, respectively, whereas for the IE-NOESY experiment the sweep widths were 6024 Hz in both dimensions. The NOE mixing time was 80 ms in the HMQC-NOE and IE-NOESY experiments. The HMQC data set consisted of 255 increments of 64 scans, that of the HMQC-NOE consisted of 200 increments of 128 scans, and that of the IE-NOESY consisted of 512 increments with 96 scans each.

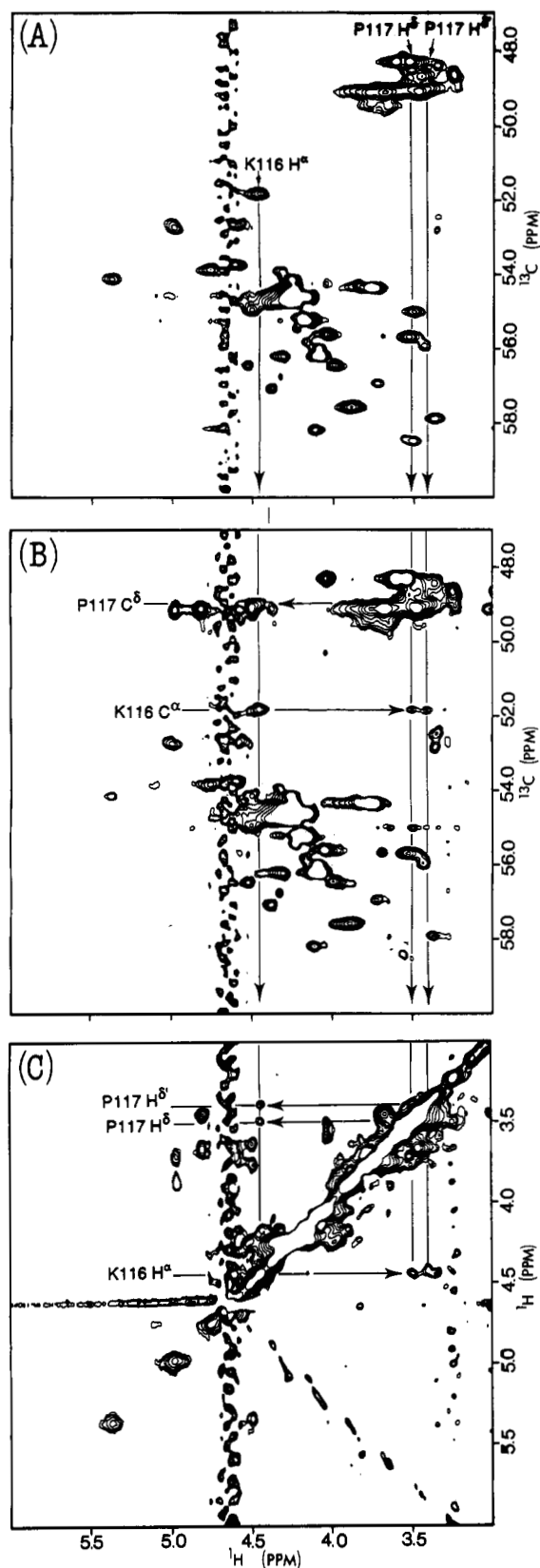


FIGURE 5: (A) HSMQC, (B) HMQC-NOE, and (C) ω_1 IE-NOESY spectra of $[\alpha\text{-}^{13}\text{C}]\text{Lys}$ and $[\beta,\delta\text{-}^{13}\text{C}]\text{Pro}$ enriched D77A+H124L. The data were collected at 37 °C on a Bruker AM500 spectrometer equipped with a $^1\text{H}/^{13}\text{C}$ variable-temperature probe. The sweep widths in F2 and F1 for the HSMQC and HMQC-NOE experiments were 6024 and 6288 Hz, respectively, whereas for the IE-NOESY experiment the sweep widths were 6024 Hz in both dimensions. The NOE mixing time was 80 ms in the HMQC-NOE and IE-NOESY experiments. The HMQC data set consisted of 407 increments of 48 scans, that of the HMQC-NOE consisted of 425 increments of 96 scans; and that of the IE-NOESY consisted of 512 increments with 80 scans each.

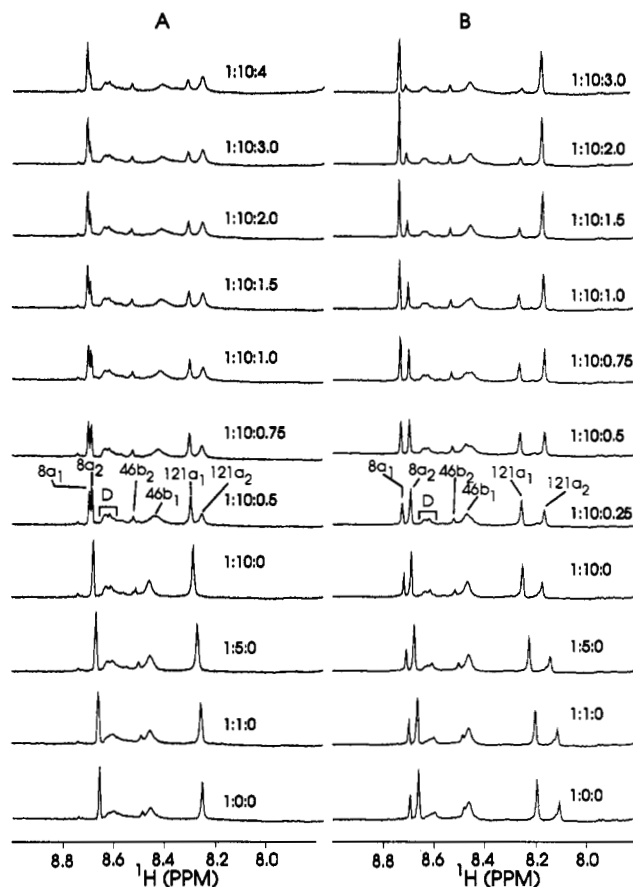


FIGURE 6: Titrations of staphylococcal nuclease mutants D77A+H124L (panel A) and G79S+H124L (panel B) with the inhibitor pdTp. The data, which were collected at 37 °C on a Bruker AM500 spectrometer, consisted of 256 scans for each point. The protein:CaCl₂:pdTp composition for each spectrum is given for each spectrum.

Lys¹¹⁶ C α (51.8 ppm), whereas a single NOE is present at the ¹³C chemical shift of Pro¹¹⁷ C δ (48.9 ppm). The NOEs arising from Lys¹¹⁶ H α have ¹H chemical shifts corresponding to the two H δ s of Pro¹¹⁷, while the NOE arising from the Pro¹¹⁷ H δ s has the same chemical shift as Lys¹¹⁶ H α . Together, the results provide convincing experimental evidence that the Lys¹¹⁶-Pro¹¹⁷ peptide bond in this mutant is predominantly *trans*.

Effect of Inhibitor Binding. Previous studies of wild-type nuclease and mutants have shown that the nucleotide inhibitor pdTp shifts the $a_1 \rightleftharpoons a_2$ equilibrium by binding preferentially to the a_1 form (Alexandrescu et al., 1989; Fox et al., 1986). A demonstration of this behavior for D77A+H124L is presented in Figure 6 (panel A). As the concentration of inhibitor is increased, the peak corresponding to the a_1 form increases at the expense of that from a_2 . To correlate these results with the Lys¹¹⁶-Pro¹¹⁷ peptide bond configuration, we repeated the same repertoire of experiments on the ternary complex of $[\alpha\text{-}^{13}\text{C}]\text{Lys}$ and $[\beta,\delta\text{-}^{13}\text{C}]\text{Pro}$ enriched D77A+H124L. Under the conditions used, the equilibrium constant for isomerization is shifted strongly toward a_1 , and the sample contains less than 14% of the a_2 form (Table I). The cross peaks indicative of the *trans* Lys¹¹⁶-Pro¹¹⁷ peptide bond are no longer present, either in the ω_1 IE-NOESY or the HMQC-NOE spectra (data not shown).

We also prepared the mutant G79S+H124L, isotopically enriched with $[\alpha\text{-}^{13}\text{C}]\text{Lys}$ and $[\alpha\text{-}^{13}\text{C}]\text{Pro}$. The Lys¹¹⁶-Pro¹¹⁷ equilibrium in this mutant (in the absence of inhibitor) is also shifted toward a_2 , although not as drastically as with D77A+H124L (Figure 1). Again, the a_1 form in G79S+H124L increases at the expense of a_2 as the inhibitor

Table I: Inhibitor Compositions of Various Samples and Equilibrium a_1/a_2 Values

protein	protein:CaCl ₂ :pdTp	a_1/a_2
H124L	1.0:0.0:0.0	14 ^a
D77A+H124L	1.0:0.0:0.0	≤0.010 ^b
D77A+H124L	1.0:20.0:10.0	6.14
G79S+H124L	1.0:0.0:0.0	0.43
G79S+H124L	1.0:1.0:0.5	1.05
G79S+H124L	1.0:2.0:1.0	2.8
G79S+H124L	1.0:10.0:5.0	8.9

^a This value is from Alexandrescu et al. (1990). ^b This number represents the lower limit of detection.

concentration is raised (Figure 6, panel B). To correlate histidine splittings with the Lys¹¹⁶-Pro¹¹⁷ peptide bond geometry, we recorded NMR spectra of [α -¹³C]Lys and [α -¹³C]Pro enriched G79S+H124L at four protein:Ca²⁺:pdTp compositions: 1:0:0, 1:1:0.5, 1:2:1, and 1:10:5. The a_1/a_2 ratios, calculated by taking the quotient of the a_1 and a_2 peak areas of His¹²¹ in the one-dimensional NMR spectrum, are reported in Table I. HSMQC and HMQC-NOE data were recorded only at the end points, but ω_1 IE-NOESY spectra were recorded at all four concentrations. NOEs indicative of the *cis* configuration were detected only in the two samples with highest inhibitor concentrations. In the spectra of the 1:10:5 complex, NOEs were observed between Lys¹¹⁶ H α and Pro¹¹⁷ H α , in both the ω_1 IE-NOESY and the HMQC-NOE experiments (Figure 1S, supplementary material).

DISCUSSION

The presence of multiple configurations of proline-containing peptide bonds in unfolded proteins has been pursued by a number of investigators and is now generally accepted as one explanation for the existence of multiple phases in the kinetics of protein folding reactions (Brandts et al., 1975; Kim & Baldwin, 1982). For folded proteins, the link between proline isomerization and multiple folded forms is less well understood, although recent results with staphylococcal nuclease (Fox et al., 1986; Alexandrescu et al., 1989) and calbindin D_{9K} (Chazin et al., 1989) indicate that structural heterogeneity due to proline isomerization may play a larger role in conformational heterogeneity among folded proteins than previously expected.

The lack of efficient means for the determination of proline configurations has hindered the investigation of their role in structure-function relationships. In place of direct methods for the detection of peptide bond configurations, indirect measures of heterogeneity are typically employed. These include chromatographic separations (Shalongo et al., 1992; Jacobsen et al., 1984), isomer-specific proteolysis (Brandts & Lin, 1986), and magnetization-transfer NMR (Evans et al., 1987) techniques. The effects of proline to glycine (Evans et al., 1987; Loh et al., 1990) or proline to alanine (Schultz et al., 1992) replacements are also often pursued. In the case of staphylococcal nuclease, magnetization-transfer studies of the separate histidine ¹H ϵ_1 signals from different forms (a_1 , a_2 , b_1 , b_2 , and unfolded forms; Evans et al., 1987; Alexandrescu et al., 1989) and the removal of histidine splittings by proline to glycine mutations (Evans et al., 1987; Loh et al., 1990) have provided persuasive evidence for the role of proline isomerization in conformational heterogeneity of the enzyme.

However, to date, there has been no direct structural evidence to support this contention. Two of the three published crystal structures have been of the wild-type protein complexed

with Ca²⁺ and pdTp (Cotton et al., 1979; Loll & Lattman, 1989); they are not expected to display heterogeneity at the Lys¹¹⁶-Pro¹¹⁷ peptide bond since the NMR results clearly demonstrate that pdTp binding shifts the equilibrium to the *cis* folded form. Only the structure of WT in the absence of active site ligands (which shows approximately 10% of the a_2 form by NMR under the crystallization conditions used; Alexandrescu et al., 1989) is expected to show any detectable heterogeneity. Since no electron density corresponding to the *trans* configuration was identified (Hynes & Fox, 1991), either the wild-type protein is fully *cis* in the crystalline state or the X-ray method was incapable of detecting the small proportion of nuclease with a *trans* Lys¹¹⁶-Pro¹¹⁷ peptide bond.

The most promising approach for the determination of prolyl peptide configurations follows from the results of Torchia et al. (1989) and Archer et al. (1993), who incorporated [α -¹³C]-Pro and [γ -¹³C]Pro and used isotope-edited NMR techniques (Otting & Wüthrich, 1990) to probe the configuration of each of the seven prolyl peptide bonds in staphylococcal nuclease³ and the nine prolyl peptide bonds in TGF- β 1, respectively. In concert with existing non-proline backbone and side-chain assignments, they were able to fully identify each of proline spin systems and assign them sequentially. In both instances, the same isotopically enriched samples were used to identify NOEs between specific proline residues and their preceding residues indicative of a *cis* peptide linkage (Wüthrich et al., 1984): Lys¹¹⁶-Pro¹¹⁷ in staphylococcal nuclease and Glu³⁵-Pro³⁶ in TGF- β 1. Although complete assignment of the resonances is a rigorous means for identifying prolyl peptide bond geometries, it constitutes an intense research effort which would have to be repeated for each mutant studied.

In order to circumvent this problem and provide built-in assignments of the NOE peaks, we have extended the selective isotope labeling to the residues on both sides of the peptide bond in question. Incorporation of ¹³C δ -labeled proline facilitates detection of NOEs characteristic of *trans* Xaa-Pro peptide bonds, while incorporation of ¹³C α -labeled proline facilitates detection of those NOEs characteristic of the *cis* geometry (Figure 3). In both cases, the preceding residue (Lys) is ¹³C α labeled. Provided that the Xaa-Pro peptide bond of interest is unique within the protein sequence, labeling patterns of this type will give rise to mutual intraresidue NOEs in NMR experiments based on dipolar transfer of magnetization from protons with single-bond ¹H-¹³C scalar couplings. The two experiments we have implemented for these purposes are the ω_1 IE-NOESY experiment (Otting & Wüthrich, 1990) and the HMQC experiment with an NOE relay (HMQC-NOE; Shon & Opella, 1989). One advantage of the HMQC-NOE experiment over the ω_1 IE-NOESY experiment is the additional ¹³C chemical shift dispersion available in the ω_1 dimension. Analysis by both experiments, however, has the advantage of assuring self-consistency among the NOEs observed.

An alternative approach would be to prepare uniformly ¹³C-labeled samples and to observe mutual interresidue NOEs indicative of the *cis* and *trans* configurations in 3D NOESY-HMQC (Marion et al., 1989) or 4D ¹³C-separated NOESY (Clare et al., 1991) experiments. The advantage of this method is the simplicity of preparing the labeled material. The disadvantages are that it requires more specialized NMR hardware than the approach used here and does not provide the built-in assignments and the same degree of spectral simplification.

The labeled amino acids needed for this study ($[\alpha\text{-}^{13}\text{C}]\text{Pro}$ and $[\beta,\delta\text{-}^{13}\text{C}]\text{Pro}^4$) were not available commercially but were prepared with relative ease by means of standard synthetic organic chemistry (Fields et al., 1954; Young & Torchia, 1983) from inexpensive precursors: $[1\text{-}^{13}\text{C}]\text{NaOAc}$, $[2\text{-}^{13}\text{C}]\text{NaOAc}$, and K^{13}CN . Specific isotopic enrichment of nuclease with $^{13}\text{C}]\text{Pro}$ and $^{13}\text{C}]\text{Lys}$ was achieved by overexpression in a strain of *E. coli* auxotrophic for proline (*proC*) and lysine (*lysA*) and catabolically deficient in proline utilization (*putPA*).

The validity of the method was tested by analysis of nuclease H124L selectively enriched with $[\alpha\text{-}^{13}\text{C}]\text{Pro}$ and $[\alpha\text{-}^{13}\text{C}]\text{Lys}$. Given that the $a_1 \rightleftharpoons a_2$ equilibrium in H124L lies far to the right ($a_1/a_2 = 14$; Alexandrescu et al., 1990; Figure 1), one anticipates observing a strong $\text{Lys H}^\alpha\text{--Pro H}^\alpha$ NOE indicative of the *cis* configuration. A single set of resonances with mutual intrasidue NOEs in the ω_1 IE-NOESY and HMQC-NOE experiments (Figure 4) confirmed this prediction. This was strengthened further by the observation that the chemical shift assignments for these resonances are fully consistent with those for nuclease H124L in the absence of active site ligands (Wang et al., 1992) and for wild-type³ nuclease (Torchia et al., 1989) as the ternary complex with Ca^{2+} and pTp .

Additional experimental evidence consistent with *cis* $\text{Lys}^{116}\text{--Pro}^{117}$ is the absence of $\text{Pro H}^\delta\text{--Lys H}^\alpha$ intrasidue NOEs in $[\alpha\text{-}^{13}\text{C}]\text{Lys}$ and $[\beta,\delta\text{-}^{13}\text{C}]\text{Pro}$ enriched H124L. Since the $a_1 \rightleftharpoons a_2$ equilibrium lies far to the right ($a_1/a_2 = 14$) and is slow on the NMR time scale, the concentration of proton pairs in what is presumably the *trans* configuration is small (0.14 mM).⁵ This is likely to be below the sensitivity limit for these experiments and is one limitation of the technique. Assuming that the limit for detection of these NOEs is 1 mM in proton pairs, then nominally, in order to detect the *trans* configuration in nuclease H124L, a sample concentration of 14 mM would be required. This corresponds to a protein concentration of 238 mg/mL, which is approximately 3-fold higher than the spectroscopically observed dimerization midpoint (Alexandrescu et al., 1989) and therefore is not experimentally feasible.

As a solution to this problem, we have monitored the $a_1 \rightleftharpoons a_2$ equilibrium in two mutants in which the equilibrium is shifted dramatically to the left (D77A+H124L and G79S+H124L; Figure 1). For $[\alpha\text{-}^{13}\text{C}]\text{Lys}$ and $[\beta,\delta\text{-}^{13}\text{C}]\text{Pro}$ enriched D77A+H124L, strong intrasidue NOEs were identified between $\text{Pro}^{117} \text{H}^\delta$ s and $\text{Lys}^{116} \text{H}^\alpha$ (Figure 5) which are diagnostic for a *trans* $\text{Lys}^{116}\text{--Pro}^{117}$ peptide bond. In the presence of inhibitor (protein: Ca^{2+} : $\text{pTp} = 1:20:10$), the a_1/a_2 composition ratio was 6.2, and these same NOEs were no longer detectable. Under these circumstances, the effective concentration of proton pairs in the a_2 form was 0.81 mM, which apparently is still below the sensitivity of the NMR experiments employed. Taken together, these data confirm that $\text{Lys}^{116}\text{--Pro}^{117}$ is *trans* in D77A+H124L and that the peptide bond equilibrium shifts toward the *cis* configuration when inhibitor is bound.

The configuration of the $\text{Lys}^{116}\text{--Pro}^{117}$ peptide bond has also been monitored in $[\alpha\text{-}^{13}\text{C}]\text{Lys}$ and $[\alpha\text{-}^{13}\text{C}]\text{Pro}$ enriched G79S+H124L. In the absence of active site ligands, the $a_1 \rightleftharpoons a_2$ equilibrium is close to unity ($a_1/a_2 = 0.43$; Figure 1;

Table I), and no intrasidue NOEs indicative of the *cis* configuration ($\text{Lys H}^\alpha\text{--Pro H}^\alpha$ NOEs) were identified. Only when sufficient inhibitor was added to shift the $a_1 \rightleftharpoons a_2$ equilibrium to $a_1/a_2 \geq 1.0$ (Table I; Figure 6) was it possible to observe a consistent set of $\text{Lys H}^\alpha\text{--Pro H}^\alpha$ NOEs (Figure 1S). The correlation between the appearance of $\text{Lys H}^\alpha\text{--Pro H}^\alpha$ NOEs and the increase in the a_1/a_2 ratio is strong evidence that the a_1/a_2 ratio reports on the *cis* \rightleftharpoons *trans* equilibrium for the $\text{Lys}^{116}\text{--Pro}^{117}$ peptide bond. As before, it is also consistent with the hypothesis that the nucleotide inhibitor binds preferentially to the *cis* folded form.

On the basis of an initial sample concentration of 2.5 mM and the fact that no NOEs were identified until a_1/a_2 exceeded 1.0, these results indicate that the concentration of the proton pairs must be ≥ 1.25 mM in order to be detected. The normal detection limit is much lower than this, which suggests that the sensitivity is being degraded by some other process. The *trans* \rightleftharpoons *cis* isomerization reaction provides an additional pathway for the leakage of magnetization. Provided that conformational exchange occurs with a rate comparable to the rate of dipolar relaxation, a significant decrease may occur since the measured NOE will be weighted by its intensity in the *trans* configuration, which is expected to be zero, or close to zero. Although a detailed analysis of the relaxation pathways has not been undertaken, inversion-transfer experiments have shown that conformational exchange in these mutants can occur on time scales comparable with dipolar cross relaxation (100–200 ms; Hinck, 1993).

Conclusions. The results presented in this paper represent the first direct structural observation of a *trans* $\text{Lys}^{116}\text{--Pro}^{117}$ peptide bond in staphylococcal nuclease. They confirm the hypothesis that the $a_1 \rightleftharpoons a_2$ conformational heterogeneity reported by histidine $^1\text{H}^{\epsilon 1}$ resonances arises from peptide bond isomerization at this site. Parallel investigations of the $b_1 \rightleftharpoons b_2$ conformational heterogeneity and its presumed link to isomerization about the $\text{His}^{46}\text{--Pro}^{47}$ peptide bond are underway.

The isotope-edited method presented here only assigns the configuration of the predominant form present in solution. The position of the *cis/trans* equilibrium is better quantified from the relative intensities of NMR peaks (such as the histidine $^1\text{H}^{\epsilon 1}$ resonances) that correspond to the individual states. The double-labeling approach is general and should find use in probing the configurations of prolyl peptide bonds in other proteins. Provided that the Xaa-Pro dipeptide of interest is unique in the protein sequence, the results immediately provide sequence-specific assignments that are independent of the state of the protein. One interesting application of this technique may be in studying prolyl peptide bonds in denatured states and in probing the contribution of residual structure to the energy of the denatured state.

ACKNOWLEDGMENT

The authors thank Dr. Janet Wood (University of Guelph) for the *proC* $\Delta(\text{putPA})$ strain of *E. coli*, the *E. coli* Genetic Stock Center (CGSC, Yale University) for lysine auxotroph AT713, and Michael Miller (University of Wisconsin) for assisting with the high-pressure hydrogenation experiments. The authors also thank Sean O'Herrin (University of Wisconsin) for advice on constructing the proline and lysine auxotroph and Dr. Ed Mooberry of the National Magnetic Resonance Facility at Madison (NMRFAM) for continuous support in NMR instrumentation. NMR spectroscopy was carried out at the National Magnetic Resonance Facility at Madison, which is supported by NIH Grant RR02301; equipment in the Facility was purchased with funds from the

⁴ $[\beta,\delta\text{-}^{13}\text{C}]\text{Pro}$ was prepared instead of $[\delta\text{-}^{13}\text{C}]\text{Pro}$ because the method of synthesis we employed utilized 1,3-dibromo[1,3- ^{13}C]propane and ethyl acetamidocyanacetate (Scheme I; Young & Torchia, 1983). The extra labeled carbon does not interfere with the strategy for detecting *cis* and *trans* Xaa-Pro peptide linkages.

⁵ This concentration was calculated by multiplying the mole fraction of the a_2 form for H124L (Table I) by the sample concentration (Experimental Procedures).

University of Wisconsin, the NSF Biological Instrumentation Program (Grant DMB-8415048), the National Biomedical Research Technology Program (Grant RR02301), NIH Shared Instrumentation Program (Grant RR02781), and the U.S. Department of Agriculture.

SUPPLEMENTARY MATERIAL AVAILABLE

Detailed descriptions of chemical syntheses; Schemes 1S and 2S showing steps in the preparation of labeled precursors 1,3-dibromo[1,3-¹³C]propane and diethyl [2-¹³C]acetamidomalonalate, respectively; Figure 1S showing HSMQC and IE-NOE spectra of the 1:10:5 complex (8 pages). Ordering information is given on any current masthead page.

REFERENCES

- Alexandrescu, A. T., Ulrich, E. L., & Markley, J. L. (1989) *Biochemistry* 28, 204–211.
- Alexandrescu, A. T., Hinck, A. P., & Markley, J. L. (1990) *Biochemistry* 29, 4516–4525.
- Archer, S. J., Bax, A., Roberts, A. B., Sporn, M. B., Ogawa, Y., Piez, K. A., Weatherbee, J. A., Tsang, M. L.-S., Lucas, R., Zheng, B., Wenker, J., & Torchia, D. A. (1993) *Biochemistry* 32, 1164–1171.
- Ausubel, F. W., Brent, R., Kensington, R. E., Moore, D. D., Seidman, J. G., Smith, J. A., & Struhl, K. (1987) *Current Protocols in Molecular Biology*, Wiley-Interscience, New York.
- Bachman, B. J. (1983) *Microbiol. Rev.* 47, 180–230.
- Barlow, D. J., & Thornton, J. M. (1988) *J. Mol. Biol.* 201, 601–619.
- Bochner, B. R., Huang, H., Schieven, G. L., & Ames, B. N. (1980) *J. Bacteriol.* 143, 926–933.
- Brandl, C., & Deber, C. M. (1986) *Proc. Natl. Acad. Sci. U.S.A.* 83, 917–921.
- Brandts, J. F., & Lin, L. (1986) *Methods Enzymol.* 131, 107–126.
- Brandts, J. F., Halvorsen, H. R., & Brennan, M. (1975) *Biochemistry* 14, 4953–4963.
- Chazin, W. J., Kördel, J., Drakenburg, T., Thulin, E., Brodin, P., Grundström, T., & Forsén, S. (1989) *Proc. Natl. Acad. Sci. U.S.A.* 86, 2195–2198.
- Clore, G. M., Kay, L. E., Bax, A., & Gronenborn, A. M. (1991) *Biochemistry* 30, 12–18.
- Cotton, F. A., Hazen, E. E., Jr., & Legg, M. J. (1979) *Proc. Natl. Acad. Sci. U.S.A.* 76, 2551–2555.
- Cuatrecasas, P., Fuch, S., & Anfinsen, C. B. (1967) *J. Biol. Chem.* 242, 1541–1547.
- Davis, R. W., Botstein, D., & Roth, J. R. (1980) *Advanced Bacterial Genetics*, Appendix I, p 207, Cold Spring Harbor Laboratory Press, Cold Spring Harbor, NY.
- Evans, P. A., Dobson, C. M., Kautz, R. A., Hatfull, G., & Fox, R. O. (1987) *Nature (London)* 329, 266–268.
- Evans, P. A., Kautz, R. A., Fox, R. O., & Dobson, C. M. (1989) *Biochemistry* 28, 362–370.
- Fields, M., Walz, D. E., & Rothchild, S. (1951) *J. Am. Chem. Soc.* 73, 1000–1002.
- Fox, R. O., Evans, P. A., & Dobson, C. M. (1986) *Nature (London)* 320, 192–194.
- Hinck, A. P. (1993) Ph.D. Thesis, University of Wisconsin, Madison, WI.
- Hynes, T. R., & Fox, R. O. (1991) *Proteins: Struct., Funct., Genet.* 10, 92–105.
- Jacobsen, J., Melander, W., Vaisnys, G., & Horváth, C. (1984) *J. Phys. Chem.* 88, 4536–4542.
- Kim, P. S., & Baldwin, R. L. (1982) *Annu. Rev. Biochem.* 51, 459–489.
- Kleckner, N., Bender, J., & Gottesman, S. (1991) *Methods Enzymol.* 204, 139–181.
- Langsetmo, K., Fuchs, J., & Woodward, C. (1989) *Biochemistry* 28, 3211–3220.
- Loh, S. N., McNemar, C. W., & Markley, J. L. (1991) in *Techniques in Protein Chemistry II* (Villafranca, J. J., Ed.) pp 275–282, Academic Press, New York.
- Loll, P. A., & Lattman, E. E. (1989) *Proteins: Struct., Funct., Genet.* 5, 183–201.
- Ludwig, M. L., & Luschinsky, C. L. (1992) in *Chemistry and Biochemistry of Flavoenzymes* (Müller, F., Ed.) Vol. III, pp 447–466, CRC Press, Boca Raton, FL.
- MacArthur, M. W., & Thornton, J. M. (1991) *J. Mol. Biol.* 218, 397–412.
- Marion, D., Kay, L. E., Sparks, S. W., Torchia, D. A., & Bax, A. (1989) *J. Am. Chem. Soc.* 111, 1515.
- Markley, J. L., Williams, M. N., & Jardetzky, O. (1970) *Proc. Natl. Acad. Sci. U.S.A.* 65, 645–651.
- Miller, J. (1977) *Experiments in Molecular Genetics*, Chapter 28, pp 201–205, Cold Spring Harbor Laboratory Press, Cold Spring Harbor, NY.
- Otting, G., & Wüthrich, K. (1990) *Q. Rev. Biophys.* 23, 39–96.
- Royer, C. A., Hinck, A. P., Loh, S. N., Prehoda, K. P., Peng, X., Jonas, J., & Markley, J. L. (1993) *Biochemistry* 32, 5222–5232.
- Sambrook, J., Fritsch, E. F., & Maniatis, T. (1989) *Molecular Cloning, A Laboratory Manual*, 2nd ed., Cold Spring Harbor Laboratory Press, Cold Spring Harbor, NY.
- Schultz, D. A., Schmid, F. X., & Baldwin, R. L. (1992) *Protein Sci.* 1, 917–924.
- Shaka, A. J., Keeler, J., & Freeman, R. (1983) *J. Magn. Reson.* 53, 313–340.
- Shalongo, W., Jagannadham, M. V., Heid, P., & Stellwagen, E. (1992) *Biochemistry* 31, 11390–11396.
- Shon, K., & Opella, S. J. (1989) *J. Magn. Reson.* 82, 193–197.
- Skelnar, V., & Bax, A. (1987) *J. Magn. Reson.* 71, 379–383.
- Stanczyk, S. M., Bolton, P. H., Dell'Acqua, M., & Gerlt, J. A. (1989) *J. Am. Chem. Soc.* 111, 8317–8318.
- Sternber, N. L., & Maurer, R. (1991) *Methods Enzymol.* 204, 19–43.
- Studier, F. W., Rosenberg, A. H., Dunn, J. J., & Dubendorff, J. W. (1989) *Methods Enzymol.* 185, 61–89.
- Torchia, D. A. (1984) *Annu. Rev. Biophys. Bioeng.* 13, 125–144.
- Torchia, D. A., Sparks, S. W., Young, P. E., & Bax, A. (1989) *J. Am. Chem. Soc.* 111, 8315–8317.
- Wang, J., Hinck, A. P., Loh, S. N., LeMaster, D. M., & Markley, J. L. (1992) *Biochemistry* 31, 921–936.
- Wang, J. F., Hinck, A. P., Loh, S. N., & Markley, J. L. (1990) *Biochemistry* 29, 102–113.
- Wüthrich, K. (1986) *NMR of Proteins & Nucleic Acids*, p 124, Wiley, New York.
- Wüthrich, K., & Grathwohl, C. (1974) *FEBS Lett.* 43, 337–340.
- Wüthrich, K., Billeter, M., & Braun, W. (1984) *J. Mol. Biol.* 180, 715–740.
- Young, P. E., & Torchia, D. A. (1983) in *Peptides: Structure & Function* (Hruby, V. J., & Rich, D. H., Eds.) pp 155–158, Pierce, Rockford, IL.
- Zuiderweg, E. R. P. (1990) *J. Magn. Reson.* 86, 346–357.